ELSEVIER

Reversible immobilization of engineered molecules by Ni-NTA chelators

J. Maly[a,b], C. Di Meo[c], M. De Francesco[c], A. Masci[c], J. Masojidek[b], M. Sugiura[d], A. Volpe[c], R. Pilloton[c,*]

[a]*Department of Biology, University of J.E. Purkyne, 40001 Usti nad Labem, Czech Republic*
[b]*Institute of Microbiology, Academy of Sciences, 379 81 Trebon, Czech Republic*
[c]*ENEA, SP061, Via Anguillarese, 301, 00060 Santa Maria di Galeria, Rome, Italy*
[d]*Osaka Prefecture University, Osaka, Japan*

Abstract

Electrochemical synthesis of nickel-nitrilotriacetic acid (Ni-NTA) chelators, for subsequent immobilization of $(His)_6$-tagged proteins (Photosystem II (PSII) as model molecule), on Au or Au-graphite electrodes is compared to chemical synthesis. Results show: (i) higher Ni-NTA surface density, (ii) shorter treatment time (1–12 min vs. 16 h normally needed for self-assembled monolayer (SAM)), (iii) possibility of addressing the chelator to only one Au electrode, in a sensor μ-array.
© 2004 Elsevier B.V. All rights reserved.

1. Introduction

Genetically modified molecules represent a powerful approach to artificial structures with improved properties for biosensor development. An original procedure, suitable for chemical immobilization of engineered $(His)_6$-tagged proteins on Au or graphite surfaces, was previously reported [2] with the result of obtaining oriented and highly specific immobilization of two engineered proteins [1]. Renewable specific binding of $(His)_6$-proteins to sensor surfaces and fast and sensitive electrochemical or optical detection of analytes were also obtained [2]. "On chip" protein pre-concentration was conveniently achieved for biosensing purposes, starting from crude unpurified extracts and avoiding protein purification steps [2]. In this paper, selective electrochemical synthesis of CYS layers on Au, Pt and graphite was studied and compared, using a model molecule (Photosystem II, PSII) with the aim of biosensors improvement.

2. Experimental

### 2.1. Preparation of Au and Au(graphite) electrodes

Au thin films were obtained by chemical deposition on Cu paths. Cu electrodes were obtained from a commercial Cu sheet deposited on fiber glass. Cu surface was lapped with SiC sheet (4000 mesh) and diamond pastes (particle size = 6 μm, then 3 μm). An impermeable dye layer, screen-printed on the copper surface, was used as a mask and $FeCl_3$ dissolved the exposed Cu, leaving the desired electrode geometries under the dye (later easily removed with acetone). Chemical Au plating on Cu was obtained with $Au(CN)_2^-$ and $Au(CN)_4^-$. An Au wire was dissolved in boiling HCl/HNO_3 (3:1) and then dried at 70–80 °C; HCl 37% was added and the solution dried again; finally, HCl 0.1 M was added to have $AuCl_3$ (0.6

g/l) in solution which was mixed with KCN (10.0 g/l), Na_2HPO_4 (6.0 g/l), NaOH (1.0 g/l), Na_2SO_3 (3.0 g/l). Gold plating was obtained by sinking the samples in the plating bath for 1 h at 70 °C; a thin Au layer (20 nm) was deposed on Cu because of the shift reaction:

$$2Au(CN)_{2 \; aq}^{-} + Cu(s) \rightarrow Cu(CN)_{4 \; aq}^{2-} + 2Au(s)$$
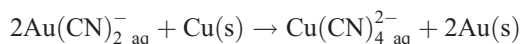
Two series of such Au electrodes were obtained and tested (Metrohm 641, Herisau, Switzerland) in a flow-cell. Series #1, with ascorbic acid at +600 mV vs. RE, gave a sensitivity of 32.3 ± 1.2 mA/M (RSD = 3.2%, $n = 3$); series #2 showed a sensitivity of 23.3 ± 2.2 mA/M (RSD = 9.8%, $n = 5$). Real surface (A_r) of Au electrodes was chronocoulometrically obtained with 0.1 mM $KFe(CN)_4$ (FeCy) in 0.1 M KCl; The two potential steps applied were, +600 and 0 mV vs. RE with 250 ms pulse width. The current signal due to FeCy reduction was plotted as Q vs. ($t^{1/2}$) and the slope of the line gave the real surface area of the Au electrode (A_r). A roughness factor of 1.13, calculated as real/geometric area ratio, was used to calculate Ni(II), CYS, and PSII surface densities reported below.

A different electrode lay-out was screen-printed by overlapping deposition of Ag (conducting paths) Ag/AgCl (RE) and graphite (WE) inks from Acheson. Graphite ink was mixed with Au(graphite) particles (10%w/w) and deposited by screen printing on a PVC sheet.

2.2. Deposition of CYS layers and synthesis of nickel-nitrilotriacetic acid (Ni-NTA chelator)

Chemical synthesis of CYS-SAM on Au was obtained in CYS 20 mM in PB for 16 h [2]. Deposition potentials of CYS on Au (0.85 V) and graphite (1.2 V) were obtained by cyclic voltammetry (CV), 0–1.4 V vs. Pt in CYS 20 mM in PB (scan rate = 50 mV/s, step potential = 10 mV); The synthesis of the Ni-NTA chelator [2] followed the common procedure: (i) glutaraldehyde 12.5% v/V in PB for 1 h, (ii) N_α-N_α-bis(carboxymethyl)-L-Lysine Hydrate (NTA) 5% w/V in PB for 1 h, (iii) $NiSO_4$ 1% w/V in distilled water for 15 min. Surface density of NTA chelator on the electrodes was electrochemically (AdCSV) determined as the Ni^{2+} content as previously described [2] with blank correction (fiber glass resin only).

2.3. Purification and immobilization of PSII

Thermophilic cyanobacterial *Thermosynechococcus elongatus* 43 H cells expressing psbC with an $(His)_6$ extension were used for purification of $(His)_6$-PSII core complexes [1]. The purified $(His)_6$-PSII core complex was immobilized on the surface of Au-CYS−NTA modified electrodes. Immobilization of PSII was obtained by incubation of electrodes in MESB containing PSII equivalent of 300 µg Chl ml^{-1} at 4 °C in complete darkness for 20 min. Prior to measurements, electrodes with immobilized PSII were thoroughly washed

with MESB. The exact amount of $(His)_6$-PSII core complex immobilized on the electrode was determined as decrease of chlorophyll concentration [4] in the solution before and after immobilization (four electrodes used in one batch in order to increase the precision of the measurement) and corrected to the blank sample (clean Au electrode). All experiments were repeated four times and average number was used for subsequent calculations.

2.4. Amperometric measurement of PSII activity

Amperometric measurement of PSII activity on the electrodes was done in a home-made flow-cell, continuously fed with MESB (flow rate 0.25 ml/min, peristaltic pump Gilson MiniPulse 3). Buffer was bubbled for 15 min with N_2 prior to starting and all through measurements. The current intensity on the WE was registered with a potentiostat and processed by AD converter and software (Oxycorder, PSI Instruments, Czech Republic). Illumination was controlled by a custom-made electronic timer, the duration was set to 1 or 5 s and light intensity about 100 µmol photons m^{-2} s^{-1}. Red and blue High Intensity light-emitting diodes (LEDs) were used.

3. Results and discussion

3.1. Electrochemical deposition of CYS on Au or Au (graphite) electrodes

CV of 10 mM CYS showed that oxidation peaks on Au and graphite electrodes decreased quickly. After few (5–10) scans the curve assumed a flat shape (Fig. 1). This means CYS is rapidly oxidized till saturation of the electrode surface. The electrochemical deposition of CYS layers on Au, thus obtained potentiostatically in 20 min, showed a rapid increase of current signal at the beginning of deposition (Fig. 2A); the shape of the 1st and 2nd derivatives (Fig. 2B) shows that current intensity quickly increases till $t = 3.3$ s ($f' =$ max and $f'' = 0$), then increases slowly till $t = 6.7$ s ($f' = 0$ and $f'' < 0$); finally current intensity decreases and steady state is reached after 30 s (f' and $f'' = 0$, $I =$ constant). The integral of current intensity (Q vs. t reported in Fig. 2C) was used to calculate surface density of CYS on Au WE, taking into account that, after Au surface was completely saturated, electrochemical reaction proceeded giving dimerisation of CYS. Ni^{+2} (513 pmol/mm^2) and NTA chelator surface densitiy, obtained with electrochemical deposition of CYS layers in 20 min resulted about 15 fold greater than that one obtained on the same material with a chemical treatment (Ni^{2+} surface density = 39 pmol/mm^2 after 16 h) and 30 fold greater than that one obtained with a chemical treatment of only 20 min. Preliminary deposition of an His-tagged alkaline phosphatase (AP) on a µ-array of gold electrodes showed that electrochemical
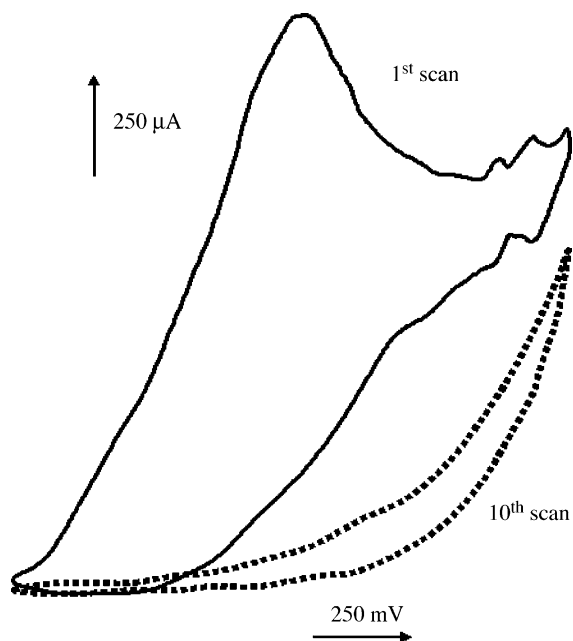
Fig. 1. Cyclic voltammetry for CYS deposition on gold (the 1st and the 10th scans) 0–1.4 V vs. Pt in CYS 20 mM in PB (scan rate = 50 mV/s, step potential = 10 mV); maximum of the peak is centered at 850 mV vs. Pt.

deposition only occurs on the chosen electrode (data not shown).

Screen-printed Au-graphite or Pt-graphite particles held the same behaviour of pure Au, allowing us to deposit CYS only on metal particles dispersed in the carbon inks at 0.85 V vs. RE, as CYS deposition on graphite electrodes occurs at higher potential (1.2 V vs. RE) (Fig. 3).

3.2. Surface density of CYS, Ni(II) and (His)$_6$-PSII

As stated above, electrochemical deposition (20 min) of CYS on Au, completely saturates electrode surface and, because Ni^{2+} combines with CYS–NTA with a stoichiometric ratio of 1:1, maximum CYS surface density results to be equal to the maximum Ni(II) surface density obtained after a 20-min electrochemical deposition (Table 1, row E = 513 pmol/mm^2, experimentally determined with adsorptive cathodic stripping voltammetry (AdCSV)). Rows A, B, C in Table 1 were obtained assuming moles of CYS $= Q(t)/nF$ with (F = 96484 C and n = 1) at t = 20,300,1200 s. The time (in row D) really needed for reaching the maximum of CYS surface density by electrochemical treatment, was interpolated from data in rows
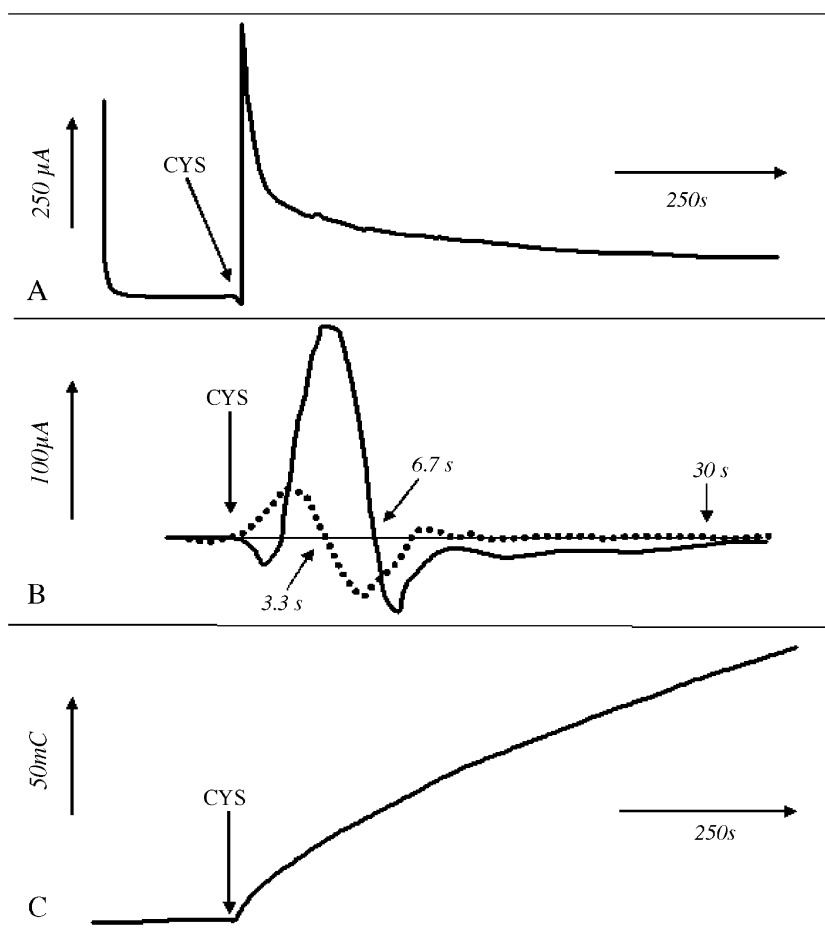

Fig. 2. Current intensity, 1st and 2nd derivatives and integral of chronoamperometric deposition of CYS on gold electrodes. (A) I(A) Peak vs. t(s) due to the CYS addition into PB to the final concentration of 20 mM, (B) dI(A)/dt(s) (continuous line) and d(dI(A)/dt(s))/dt(s) (dotted line), (C) $\int(I(A)dt(s)$.
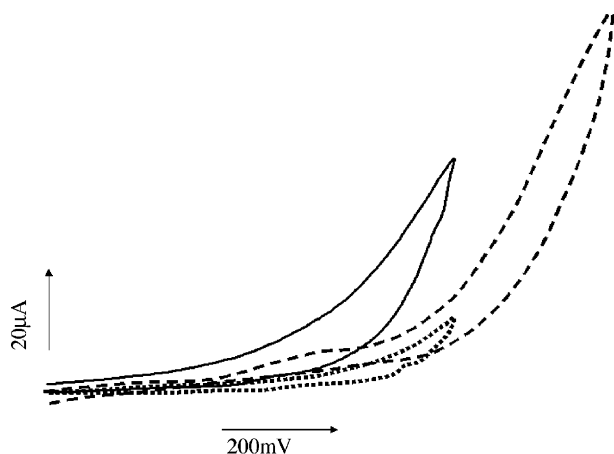
Fig. 3. Cyclic voltammetry of 20 mM CYS in PB with screen-printed electrodes. Continuous line: Au-graphite WE; dashed line: Carbon-graphite WE; dotted line: Pt-Graphite WE.

A, B, C and resulted to be $t_{max} = 711$ s ($\sim$ 12 min). Our experimental data are confirmed by comparing row E (experimental data) with (i) calculation by dimension of the ionic radius of Ni(II) (row F), (ii) calculation by dimension of the octaedral Ni(II) complex (row G), (iii) their relative magnitude and order in the series (G>E>F). Row H was calculated by considering the dimension of the PSII core crystal and row I was spectrophotometrically obtained considering the chlorophyll content of immobilized(His)$_6$-PSII. Again, experimental data from row I showed the same magnitude order of row H. Again, Ni(II) combines with (His)$_6$-PSII with a stoichiometric ratio of 1:1 so, with an electrochemical treatment of $t_{max} = 12$ min (or higher) a ratio Ni:(His)$_6$-PSII $\sim$ 39,500 was experimentally determined. This means that a single (His)$_6$-PSII

Table 1
Ni^{2+} and CYS and PSII surface densities

	Molecule	Time (s)[a]	Surface density (pmol/mm^2)	CV (%)	Method
A	Cys	20	100	4.2	CYS = Q(t)/nF
B	Cys	300	246	3.8	CYS = Q(t)/nF
C	Cys	1200	1306	5.1	CYS = Q(t)/nF
D	Cys	711 = t_{max}	513	–	interpolation from rows A,B,C for CYS = 513 (row E)
E	Ni^{2+}	1200	513	4.1	AdCSV
F	Ni^{2+}	–	400,000	–	Ni^{+2} ionic radius
G	Ni^{2+}	–	400	–	Ni(II) octaedrical complex radius
H	PSII	–	0.088	–	dimension of 2D PSII crystal
I	PSII	300	0.013	10.2	Chlorophyll content

Experimental values are compared with those obtained with theoretical calculation.

[a] Treatment time for electrochemical deposition of CYS-SAM on Au.

covers $\sim$ 39,500 Ni(II) heads but binds only one of them through the His$_6$-tag. So, certain amount of this chelator could be substituted with other functional groups or molecules, still obtaining the same surface density of immobilized (His)$_6$-PSII. In our opinion, mixed layers consisting of different thiol molecules immobilized onto the surface, will improve performance of biosensors (i.e. conductive molecular wires for direct electron transfer to the electrodes or hydrophobic chains [3] of OCT to inprove diffusion of hydrophobic mediators) as reported in the following section.

3.3. Comparison of the PSII monolayer versus the cross-linked PSII in a bovine serum albumin (BSA)–Ga matrix

The higher Ni^{2+} surface density obtained with electrochemical deposition of CYS on the electrode surface was not responsible of higher peaks respect to the chemically deposited ones as reported in Fig. 4, where the reoxidation rate of the reduced form of the electron acceptor is shown for CYS–NTA–PSII (chemically and electrochemically deposited) and crosslinked PSII (e.g using the BSA–GA matrix [5,6]). On the contrary, the lower peak could be explained with the redundant number of Ni^{+2} heads that does not reflect in a significant increase of PSII molecules on the electrode surface. In addition, electrochemically deposited CYS layers should be very different in structure from chemically assembled ones because of fast rate of deposition that does not allow for preliminary self-assembling. In our opinion, electrochemically deposited CYS layers should be described as disordered, compact and rigid multilayers (electrochemically deposited multilayers, EDM, in contrast with self-assembled monolayers, SAM) which significantly affect diffusion toward the electrode. The height of the peaks depends on the different quantity of PSII immobilized on the gold electrode, while reoxidation rate is strictly related to the ability of the mediator to diffuse through the immobilized layers. In the first case, a
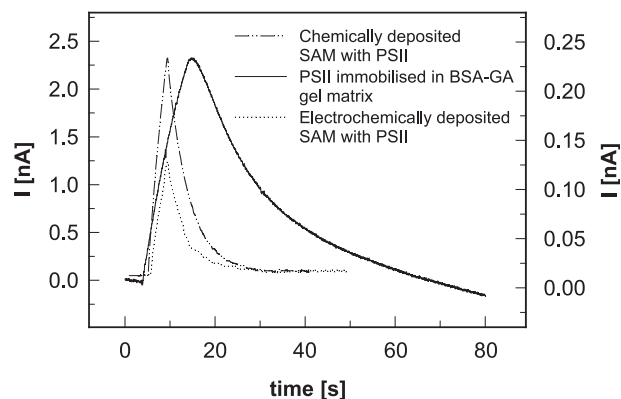

Fig. 4. Current response of the PSII on Au WE. After illumination (5 s) current increases due to the reoxidation of the artificial electron acceptor (duroquinone). Data obtained with three different immobilization methods on Au screen-printed WE.

great amount of PSII is entrapped and cross-linked in a dense diffusion layer of BSA−GA, in the second ones, it is free in solution and linked to the electrode surface through the his-tag and the NiNTA chain.

In the case of PSII monolayer immobilized on a CYS-EDM, a rapid, nearly immediate inhibition of PSII electrode was observed directly after the addition of herbicide because of the narrow diffusion layer for reduced electron acceptor (DQ) and exposition of the active PSII out to the buffer solution and the inhibitor. On the contrary, for BSA−GA−PSII gel matrix a stable signal of inhibited electrode is obtained after 15 min of herbicide exposure. I_{50} value of 3 different type of electrodes was then compared for atrazine. Au−CYS−NTA−PSII electrode showed a slight change ($I_{50} = 2 \times 10^{-8}$ M) compared to the electrode with BSA−GA−PSII gel matrix ($I_{50} = 9 \times 10^{-8}$ M). A striking difference ($I_{50} = 5 \times 10^{-10}$ M), compared to the previous two, has been observed in the third electrode type consisting of a mixed layers (CYS + OCT) with increased hydrophobic properties. The strategy depicted at the end of the previous section, regarding the possibility to deposit mixed layers together with Ni-NTA chelators will be further investigated to obtain increased performances of this biosensor.

4. Conclusions

Electrochemical formation of CYS layers on Au electrode surface occurred at 0.85 V vs. RE and resulted in a shorter treatment time (12 min vs. 16 h of chemical treatment) and in higher Ni^{+2} surface density. Electrochemical deposition of CYS on Au-graphite composite electrodes occurred at 0.85 V vs. RE, allowing deposition of CYS only on the metal particles, because of the higher potential (1.2 V) needed on graphite electrodes. Additionally, preliminary experiments with HIS-tagged AP showed the possibility to electrochemically address the synthesis of the chelator, to only one Au electrode in a sensor μ-array.

The difference in shape and in height of the signal, due to PSII activity in chemically and electrochemically deposited CYS layers, suggested also a difference in the structure of these layers. For this reason we suppose that our CYS film have not to be considered as a SAM but as an electrochemically deposed multilayer (EDM).

The redundant number of Ni^{+2} heads available for (His)$_6$-tagged proteins was then decreased and mixed layers were deposited onto the electrode surface, obtaining better performances of the biosensor in terms of substrate diffusion.

References

[1] M. Sugiura, Y. Inoue, Highly purified thermo-stable oxygenevolving photosystem II core complex from the thermophilic cyanobacterium *Synechococcus elongatus* having His-tagged CP43, Plant Cell Physiol. 40 (1999) 1219–1231.

[2] J. Maly, E. Illiano, M. Sabato, M. De Francesco, V. Pinto, A. Masci, D. Masci, J. Masojidek, M. Sugiura, R. Franconi, R. Pilloton, Immobilisation of engineered molecules on electrodes and optical surfaces, Mater. Sci. Eng., C, Biomim. Mater., Sens. Syst. 22 (2002) 257–261.

[3] R. Garjonyte, A. Malinauskas, Amperometric glucose biosensors based on Prussian Blue polyaniline-glucose oxidase modified electrodes, Biosens. Bioelectron. 15 (2000) 445–451.

[4] D.I. Arnon, Copper enzymes in isolated chloroplasts. Polyphenoloxidase in *Beta vulgaris*, Plant Physiol. 24 (1949) 1–15.

[5] M. Koblizek, J. Komenda, T. Kucera, J. Masojidek, R. Pilloton, A.K. Mattoo, M.T. Giardi, A sensitive Photosystem II-based biosensor for detection of a class of herbicides, Biotech. Bioeng. 60 (1998) 664–669.

[6] M. Koblízek, J. Malý, J. Masojídek, J. Komenda, T. Kucera, M.T. Giardi, A.K. Mattoo, R. Pilloton, A biosensor for the detection of triazine and phenylurea herbicides designed using Photosystem II coupled to a screen printed electrode, Biotech. Bioeng. 78 (2002) 110–116.